

Numerical analysis of CO₂ capture efficiency in post combustion CCS technology in terms of varying flow conditions

PAWEŁ NIEGODAJEW
DARIUSZ ASENDRYCH*
STANISŁAW DROBNIAK

Częstochowa University of Technology, Armii Krajowej 21,
42-200 Częstochowa, Poland

Abstract The paper deals with the computational fluid dynamics modelling of carbon dioxide capture from flue gases in the post combustion-capture method, one of the available carbon capture and storage technologies. 30% aqueous monoethanolamine solution was used as a solvent in absorption process. The complex flow system including multiphase countercurrent streams with chemical reaction and heat transfer was considered to resolve the CO₂ absorption. The simulation results have shown the realistic behaviour and good consistency with experimental data. The model was employed to analyse the influence of liquid to gas ratio on CO₂ capture efficiency.

Keywords: CO₂, CCS, Post-combustion capture, Chemical absorption, CFD

Nomenclature

- a – surface area, m²/m³
- A – cross sectional area of absorber column, m²
- C – molar concentration, kmol/m³
- C_s – constant in Eq. (5)
- E_r – enthalpy source term, W/m³
- F – phase interaction force, N/m³

*Corresponding Author. E-mail: darek@imc.pcz.czyst.pl

g	–	gravitational acceleration, m/s^2
G	–	mass flux of gas phase, kg/s
h	–	specific enthalpy, J/kg
h_l	–	liquid holdup, m^3/m^3
J	–	flux of species diffused, $\text{kg}/(\text{m}^3\text{s})$
k_f	–	forward reaction rate constant, $\text{m}^3/(\text{kmol s})$
L	–	mass flux of liquid phase, kg/s
M	–	molecular weight, kg/kmol
M_B	–	momentum sink term in porous zone, N/m^3
p	–	static pressure, Pa
Q	–	heat flux exchanged between phases, W/m^3
Q	–	CO_2 mass flux, kg/s
R	–	heterogeneous reaction rate, $\text{kg}/(\text{m}^3\text{s})$
R	–	mass source term, $\text{kg}/(\text{m}^3\text{s})$
t	–	time, s
T	–	temperature, K
u	–	velocity, m/s
V	–	volume flux, m^3/s
y	–	axial coordinate, m
Y	–	mass fraction, kg/kg

Greek symbols

α	–	volume fraction, m^3/m^3
α	–	CO_2 loading, $\text{mol CO}_2/\text{mol MEA}$
λ	–	thermal conductivity, $\text{W}/(\text{m K})$
ε	–	porosity, m^3/m^3
η	–	CO_2 capture efficiency, %
μ	–	dynamic viscosity, Pa s
ξ	–	drag coefficient
ρ	–	density, kg/m^3

Subscripts

CO_2	–	carbon dioxide
g, l	–	gas/liquid phase
in, out	–	inlet to/outlet from the absorber
MEA	–	monoethanolamine

Abbreviations

CCS	–	Carbon Capture and Storage
CFD	–	Computational Fluid Dynamics
ICHPW	–	Institute for Chemical Processing of Coal
PCC	–	Post Combustion Capture

1 Introduction

Carbon dioxide removal from flue gases in post-combustion capture (PCC) method is regarded as the most matured technique for the CO₂ separation among available CCS (carbon capture and storage) technologies. This approach has been tested in a laboratory-scale [1], pilot plant installations [2–5] and has been even scaled up to demonstration plant level [6]. With PCC technology carbon dioxide is separated from flue gases by chemical absorption (one of the options) with the use of an aqueous solvent solution in absorber column (see Fig. 1). The process is reversed in a stripper, allowing to release captured CO₂ which is then compressed and transported to the storage location [7]. Monoethanolamine (MEA) is the most widely used solvent in PCC, generally due to its high reactivity and commonly available comprehensive database of its physical properties [3]. PCC is also the most flexible solution among CCS technologies as it can be applied to almost every existing power plant with no need of its redesign. The only requirement is to provide additional room for its CCS installation.

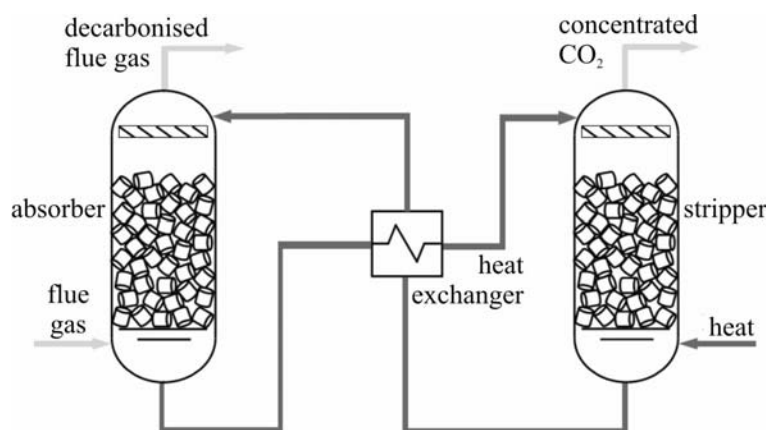


Figure 1. General process flow diagram for PCC technology.

Continuously growing progress in CCS technology enforces an implementation of new more efficient solutions and that is why the experimental research studies have to be supported by numerical analyses of this complex process. Numerical modeling can help testing the feasibility of novel techniques towards their applications to industrial conditions. A number of studies related to PCC modelling has been published over the recent decade. These works focus on numerical modeling by means of simplified 0D com-

mercial codes, mainly ASPEN [8,9] and gPROMS [10,11] or 1D models [12]. These approaches have, however, limited capabilities as they do not allow for an insight into the details of the process. The computational fluid dynamics (CFD) is able to overcome these limitations as a numerical tool enabling to perform the advanced simulations of thermo-hydrodynamic phenomena combined with absorption chemistry.

In the present paper the previously developed CFD model of CO₂ capture in the absorber column [7] is applied for the analysis of the process efficiency. CO₂ absorption has to be regarded as a complex system of physicochemical phenomena including hydrodynamics of countercurrent gas-liquid flow in porous region, chemical reaction and thermal effects due to its highly exothermic character. The research is performed in cooperation with the Institute for Chemical Processing of Coal (IChPW) in Zabrze where the small-scale laboratory PCC facility is installed. The results of experimental trials [1] were used as a reference for validation of the numerical model of the carbon dioxide capture process.

2 Model description

2.1 Problem formulation

The present work focuses on the CO₂ absorption process being the first part of PCC technology, so it neglects the stripper section responsible for the CO₂ release from loaded amine solution. Geometry of the computational domain corresponds to the reference IChPW installation [1]. The detailed description of the numerical model and the boundary conditions can be found in [7]. The 30% aqueous solution of monoethanolamine (MEA), a primary amine, was used in CO₂ separation process. The actual material properties (density, viscosity) of MEA were taken from [13] as the functions of temperature, CO₂ loading (number of moles of CO₂ per mole of amine) and mass MEA fraction in liquid mixture. The operating parameters of PCC process applied during simulation (and following the experimental conditions) are collected in Tab. 1.

Aqueous MEA solution supplied at absorber inlet did not include absorption products (i.e., CO₂ loading was equal to 0) as their actual content in the liquid was not available at the IChPW test facility. It should be noted, however, that in the real installations the solvent entering the absorber column contains certain portion of loaded MEA [19,20] influencing the entire process performance.

Table 1. The operating parameters of the CO₂ capture process and their ranges applied during simulations.

Parameter	Symbol	Unit	Value
liquid mass flux	L	kg/h	18.3–59.7
liquid temperature	T_l	K	298.5–316.3
gas mass flux	G	kg/h	7.13–8.03
gas temperature	T_g	K	290.3–299.9
CO ₂ mass fraction	Y_{CO_2}	%	10.5–12.7
CO ₂ loading at inlet	α	mol CO ₂ /mol MEA	0
power supplied in stripper	–	W	3000

2.2 Governing equations

A two-fluid Euler-Euler multiphase approach was implemented to describe countercurrent gas-liquid flow in a packed bed. In this model conservation equations are formed for each phase separately. The conservation of mass for k th phase can be written in a form

$$\frac{\partial}{\partial t}(\alpha_k \rho_k) + \nabla(\alpha_k \rho_k \vec{u}_k) = R_k, \quad (1)$$

where u_k is the velocity vector, ρ_k phase density, α_k denotes void fraction and R_k is the mass source term corresponding to species production/destruction due to chemical reaction. The conservation of momentum for k th phase with respect to the Eulerian multiphase model (for incompressible flow) has the following form:

$$\begin{aligned} \frac{\partial}{\partial t}(\alpha_k \rho_k \vec{u}_k) + \nabla(\alpha_k \rho_k \vec{u}_k \vec{u}_k) = \\ = -\alpha_k \nabla p + \nabla^2(\alpha_k \mu_k \vec{u}_k) + \alpha_k \rho_k \vec{g}_k + \vec{M}_{B,k}, \end{aligned} \quad (2)$$

where p is a static pressure shared by all phases, μ_k stands for dynamic viscosity and g_k is a gravity vector. In the porous region, being the most important absorber column section, the additional flow resistance, $M_{B,k}$, occurs. This resistance is calculated according to the theory developed and verified by numerous experimental data sets by Billet [14]. It provides the description of the most important packed bed characteristics as the functions of packing elements parameters, fluids properties as well as the fluxes of both phases. The relationship between the liquid holdup, h_l , and

the drag coefficient ξ_g for gas phase is given by the following formula:

$$a^2 \mu_l \frac{V_l}{A} = h_l^{1/n} \left(\frac{g}{3} \rho_l - \frac{\xi_g}{4} \frac{a}{A h_l (\varepsilon - h_l)^2} \frac{V_g^2}{A^2} \rho_g \right), \quad (3)$$

where V denotes volumetric flowrate. Value of n for laminar flow regime has been found to be [14]:

$$n = 1/3. \quad (4)$$

Liquid holdup and drag coefficient are unknown in principle. In order to solve Eq. (3) it is necessary to supplement the system with additional empirical equation. According to the extensive experimental data, Billet [14] has proposed the following formula for the drag coefficient:

$$\xi_g = \frac{g}{C_s^2 \left[\frac{L}{G} \sqrt{\frac{\rho_g}{\rho_l}} \left(\frac{\mu_l}{\mu_g} \right)^{0.4} \right]^{-0.652}}. \quad (5)$$

The above relationship has been found to have general character, i.e., it can be applied for calculations of various types and sizes of packing elements. Constant C_s is used to fit the formula to the particular packed bed.

As far as the reacting system is considered, the additional governing transport equations of i th species must be included in the model

$$\frac{\partial}{\partial t} (\alpha_k \rho_k Y_{i,k}) + \nabla (\alpha_k \rho_k \vec{u}_k Y_{i,k}) = -\nabla \alpha_k \vec{J}_{i,k} + R_i, \quad (6)$$

where $Y_{i,k}$ is the mass fraction, $J_{i,k}$ is the diffused flux of the i th species and R_i stands for the heterogeneous reaction rate, i.e., the mass flux of particular species produced/destroyed due to the reaction.

To describe the energy transfer in Eulerian model, a separate enthalpy equation is solved for k th phase

$$\frac{\partial}{\partial t} (\alpha_k \rho_k h_k) + \nabla (\alpha_k \rho_k \vec{u}_k h_k) = \alpha_k \frac{\partial p}{\partial t} + \nabla (\lambda_k \nabla T_k) + Q_k + E_{k,r}, \quad (7)$$

where h_k is the specific enthalpy, λ_k stands for thermal conductivity, Q_k is the intensity of heat exchange between phases and $E_{k,r}$ is the enthalpy source term due to chemical reaction.

The chemistry of CO₂ absorption by aqueous MEA solution is usually described by the system of several equilibrium reversible reactions. However, for the temperatures and media compositions applied in absorber

columns the process may be treated as a nonreversible and described by the following single reaction [6,15,16]:



leading to formation of carbamate and protonated MEA molecules. In above reaction R represents an alcanol group $(\text{CH}_2)_2\text{OH}^-$. The reaction rate (mass flux) of i th chemical species produced/destroyed due to the heterogeneous second-order reaction is given by

$$R_i = M_i k_f C_{\text{MEA}} C_{\text{CO}_2}, \quad (9)$$

where M_i is the molecular weight, k_f is a forward reaction rate constant and C_{MEA} and C_{CO_2} stand for molar concentrations of reacting media, i.e., MEA and carbon dioxide, respectively. The following experimentally based expression [17]:

$$\log(k_f) = 10.99 - 2152/T \quad (10)$$

was adopted to describe the reaction rate constant.

2.3 Numerical tools and procedure

The simulations were performed with use of commercial software ANSYS FLUENT v.13 [18]. The Eulerian/Eulerian multiphase model has been adopted to describe the countercurrent two-phase flow in a porous zone. The second order discretization schemes were applied to Navier-Stokes equations and the SIMPLE algorithm [19] was used for the velocity-pressure coupling.

The computational domain was generated and discretized by the ANSYS GAMBIT preprocessor [20]. The computational mesh has been produced as a result of a series of tests with grids of different sizes and meshing strategies. The final mesh has been generated in two-step procedure including mesh adaptation in sensitive regions. More detailed information about the applied mesh and its generation can be found in [21].

3 Results

The CFD model presented in the previous chapter was employed to perform a series of simulations of the carbon dioxide absorption process with the use of 30% aqueous monoethanolamine solution. Input parameters applied in the model corresponded exactly to the experimental test trials performed

at IChPW on the laboratory installation [1]. The crucial parameter from the viewpoint of CO₂ capture efficiency, i.e., liquid to gas ratio was varied in a relatively wide range $L/G = 2.5\text{--}7.4$ kg/kg.

At first the distributions of process key parameters along a column axis were analysed for the $L/G \approx 4.46$. As it was shown in [7] the flow in a packed bed is practically free from wall effects, so the axial distributions are fully representative to the entire absorber. Figure 2 presents the profiles of species concentration (Fig. 2a), temperatures (Fig. 2b) and reaction rate (Fig. 2c). In Fig. 2a all the species taking part in the reaction (see Eq. (8)) are included, i.e., reagents and products:

- carbon dioxide – CO₂,
- monoethanolamine – MEA,
- protonated MEA – MEA-H,
- MEA carbamate – MEA-CO₂.

Aqueous monoethanolamine solution is supplied from the source located above the porous zone region with 30% MEA mass fraction. In porous zone unloaded MEA concentration decreases due to its reaction with CO₂ flowing countercurrently and reaches the value about 22% at the bottom of packing section. Carbon dioxide profile indicates opposite trend as it is supplied at the bottom of the absorber, and its mass fraction drops from initial value of 12.1% to 0.7% at the outlet. It should be noted that the 90% capture efficiency was achieved with the use of approx. one fifth of MEA entering the absorber. Such a significant amount of excessive MEA at the inlet is necessary to maintain the reactivity of the process at the high level even at the bottom of the absorber column where the highest concentration of loaded MEA occurs (see Fig. 2a). Additionally in Fig. 2a mass fractions of MEA products are presented, namely MEA-H and MEA-CO₂. The molar fractions of both reaction products must be equal as it implies from the stoichiometry of the absorption reaction (see Eq. (8)). However, the mass fractions differ quantitatively due to different molar masses.

Figure 2b presents the temperature distributions of both phases. It can be seen that gas phase is strongly heated by the liquid at the bottom of the column and both temperature profiles collapse into one curve just above the bottom of the packed bed. It indicates how effective is the interphase heat exchange in the porous zone of the strongly enlarged contact area. As a complement, the distribution of reaction rate along the absorber axis is presented in Fig. 2c. Reaction rate rises with decreasing axial position as the

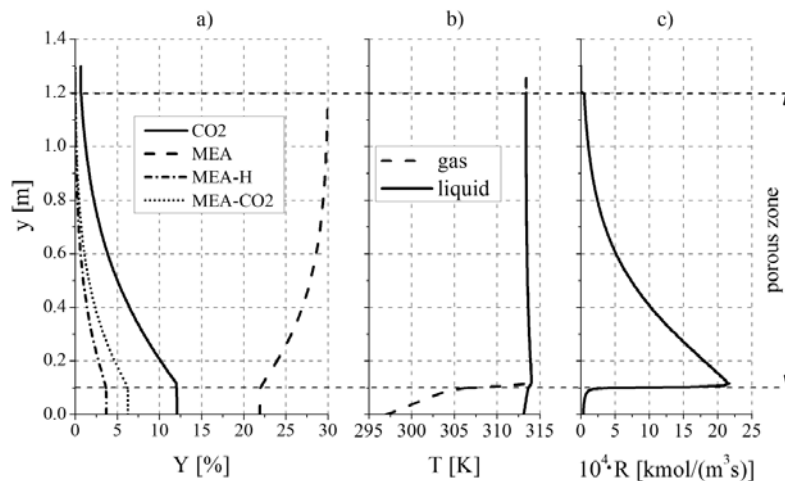


Figure 2. Axial distributions of mass fractions of reactants and products (a), media temperatures (b) and reaction rate (c).

concentration of CO₂ increases (see Fig. 2a) and reaches its maximum level at the bottom of porous zone. Therefore, when liquid leaves the packing section the reaction rate value falls down what can be explained by the acceleration of aqueous MEA solution and significant reduction of its volume fraction in this region.

From the practical point of view the most important parameter of absorber column in PCC technology is a CO₂ capture efficiency defined as

$$\eta = \frac{Q_{in} - Q_{out}}{Q_{in}} 100\% , \quad (11)$$

where Q_{in} and Q_{out} are CO₂ mass fluxes at the absorber inlet and outlet, respectively. The dependence of CO₂ capture efficiency on liquid to gas ratio (L/G), representing the mass fluxes of both phases is shown in Fig. 3 together with the corresponding experimental data collected from the laboratory installation [1]. One can easily notice that the capture efficiency rises with the increasing L/G ratio for both sets of data, i.e., the experimental data and simulation results. The rise of the CO₂ capture efficiency can be correlated with the mean (averaged within the column) liquid holdup distribution presented in Fig. 4a. One may easily notice approx. 50% holdup growth within the L/G range under consideration. The higher the liquid holdup the higher the molar concentration of unloaded amine C_{MEA} , and in turn the faster the reaction rate (see Eq. (9)).

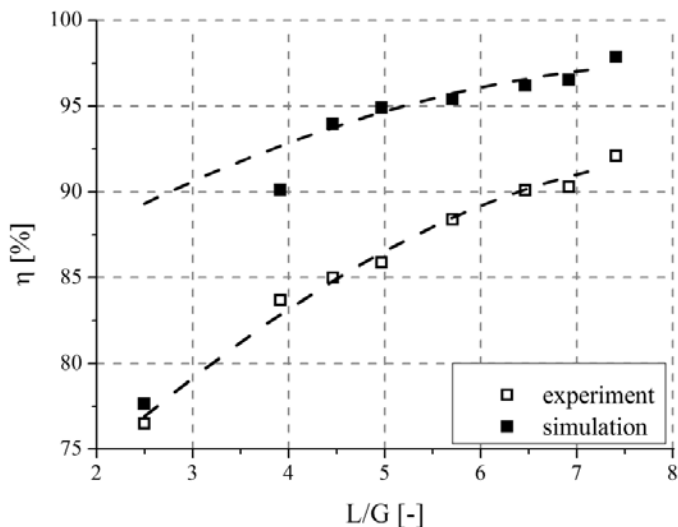


Figure 3. CO₂ capture efficiency as a function of liquid to gas ratio – comparison of simulation and experimental data.

Although both $\eta(L/G)$ profiles indicate the same increasing tendency it is well visible that simulation noticeably overpredicts the experimental data. Both distributions were approximated with the best-fit curves (see dashed lines in Fig. 3) which tend to saturate at the same level close to 100%. It should be noted that for the simulation data the best-fit distribution was produced excluding the efficiency values corresponding to $L/G \approx 2.5$ and $L/G \approx 4$. As it implies from previous simulation work [7] conducted with the same numerical approach and 20% aqueous MEA solution the discrepancies between numerical data and experimental results grow with decreasing L/G . Capture efficiencies simulated for $L/G \leq 4$ clearly deviate from that scenario, and that is why they were excluded from the best-fit approximation. The analysis of data acquired at the IChPW installation allowed to find out that for these lowest L/G ratios the temperatures of flue gases entering the absorber were significantly lower than for the remaining test cases as shown in Fig. 4b. Starting from the case $L/G \approx 4.4$ inlet gas temperatures indicate slight scatter around the mean level of approx. 314.2 K, shown in Fig. 4b with a dashed line. The temperature differences between that level and the test cases corresponding to the lowest L/G are significant, i.e., 10.5 deg for $L/G \approx 2.5$ and even 15.5 deg for $L/G \approx 4$, so that is the reason for the slowed down reaction rate (see Eq. (10)) and in turn for

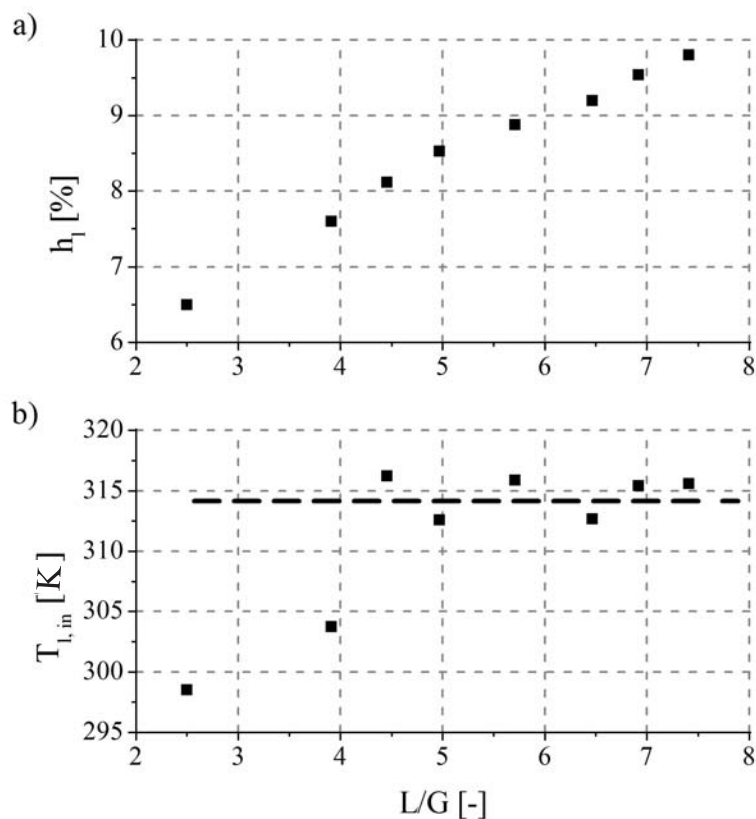


Figure 4. Theoretical liquid holdup calculated according to Billet [14] (a) and the flue gases temperature entering the IChPW installation (b) versus liquid to gas ratio.

reduced capture efficiency.

Coming back to the discrepancies between the numerical and experimental data collected in Fig. 3, they can be explained with different composition of amine solution at the absorber inlet. As it is known from literature (see, e.g., [22,23]) the amine solvent entering the absorber section contains significant portion of loaded MEA. However, these data were not available from the IChPW CCS facility, so it was not possible to set correctly (i.e., corresponding to experiment) the boundary conditions in numerical computations. Instead, the assumption was made about the absence of loaded MEA in the absorber inlet. As a consequence one may expect the artificial enhancement of the system reactivity (see Eq.(9)) leading to the overpre-

diction of CO₂ capture efficiency. One could expect that the increase of the liquid inlet temperature up to the level of 314.2 K should move the simulation data points in Fig. 3 onto the best-fit line.

4 Conclusions

A computational fluid dynamics model has been applied to perform a series of simulations of carbon dioxide capture process from flue gases by chemical absorption with use of 30% aqueous monoethanolamine solution. A complex physicochemical system including two-phase gas-liquid flow hydrodynamics, heat transfer and absorption chemistry has been used and examined under the operating conditions of laboratory-scale absorber column. Simulation results have been found to be in a good consistency with experimental data showing its usefulness to practical applications. The series of simulations allowed to formulate the following observations:

- The CFD model is capable to perform a detailed CO₂ capture analysis and provide an insight into the partial processes and their mutual interactions.
- The CO₂ capture efficiency has been found to strongly depend on the liquid to gas ratio (L/G) – the key process parameter.
- The discrepancies between the experimental and numerical results are most likely caused by the presence of loaded MEA at laboratory absorber inlet, while neglected in the CFD simulation.

Acknowledgements The results presented in this paper were obtained from research work co-financed by the National Centre of Research and Development in the framework of Contract SP/E/1/67484/10 – Strategic Research Programme – Advanced technologies for energy generation: Development of a technology for highly efficient zero-emission coal-fired power units integrated with CO₂ capture.

Project DoktoRIS is acknowledged for providing the scientific scholarship to Mr. Niegodajew.

Received 14 October 2013

References

- [1] KRÓTKI A., WIĘCŁAW-SOLNY L., TATARCZUK A., WILK A., ŚPIEWAK D.: *Laboratory studies of CO₂ absorption with the use of 30% aqueous monoethanolamine solution*. Arch. Combust. **12**(2012), 195–203.
- [2] MOSER P., SCHMIDT S., WALLUS S., GINSBERG T., SIEDER G., CLAUSEN I., PALACIOS J.G., STOFFREGEN T., MIHAILOWITSCH D.: *Enhancement and long-term testing of optimised post-combustion capture technology – Results of the second phase of the testing programme at the Niederaussem pilot plant*. Energy Procedia **37**(2013), 2377–2388.
- [3] MOSER P., SCHMIDT S., SIEDER G., GARCIA H., STOFFREGEN T.: *Performance of MEA in long-term test at the post-combustion capture pilot plant in Niederaussem*. Int. J. Greenh. Gas Con. **5**(2011), 620–627.
- [4] SØNDERBY T.L., CARLSEN K.B., FOSBØL P.L., LARS KIØRBOE G., VON SOLMS N.: *A new pilot absorber for CO₂ capture from flue gases: Measuring and modelling capture with MEA solution*. Int. J. Greenh. Gas Con. **12**(2013), 18–192.
- [5] DUGAS R., ALIX P., LEMAIRE E., BROUTIN P., ROCHELLE G.: *Absorber model for CO₂ capture by monoethanolamine application to CASTOR pilot results*. Energy Procedia **00**(2008), 103–107.
- [6] JAYARATHNA S., LIE B., MELAAEN M.C.: *Development of a dynamic model of a post combustion CO₂ capture process*. Energy Procedia **37**(2013), 1760–1769.
- [7] ASENDRYCH D., NIEGODAJEW P., DROBNIAK S.: *CFD modelling of CO₂ capture in a packed bed by chemical absorption*. Chem. Process Eng. **34**(2013), 1, 269–282, DOI: 10.2478/cpe-2013-0022.
- [8] ALIE C.: *CO₂ Capture With MEA: Integrating the Absorption Process and Steam Cycle of an Existing Coal-Fired Power Plant*. MSc thesis, University of Waterloo, Waterloo, Ontario 2004.
- [9] KOTHANDARAMAN A., NORD L., BOLLAND O., HERZOG H.J., MCRÆE G.J.: *Comparison of solvents for post-combustion capture of CO₂ by chemical absorption*. Energy Procedia **1**(2009), 1373–1380.
- [10] LAVAL A., WANG M., STEPHENSON P., KOUMPOURAS G., YEUNG H.: *Dynamic modelling and analysis of post-combustion CO₂ chemical absorption process for coal-fired power plants*. Fuel **89**, 2010, 2791–2801.
- [11] HARUN N., DOUGLAS P.L., RICARDEZ-SANDOVAL L., CROISSET E.: *Dynamic simulation of MEA absorption processes for CO₂ capture from fossil fuel power plant*. Energy Procedia **4**(2011), 1478–1485.
- [12] SIMON L.L., ELIAS Y., PUXTY G., ARTANTO Y., HUNGERBUHLER K.: *Rate based modeling and validation of a carbon-dioxide pilot plant absorption column operating on monoethanolamine*. Chem. Eng. Res. Des. **89**(2011), 9, 1684–1692.
- [13] WEILAND R.H., DINGMAN J.C., CRONIN D.B., BROWNING G.J.: *Density and viscosity of some partially carbonated aqueous alkanolamine solutions and their blends*. J. Chem. Eng. Data **43**(1998), 378–382.
- [14] BILLET R.: *Packed Towers in Processing and Environmental Technology*. VCH Verlagsgesellschaft mbH, Weinheim 1995.

- [15] ABOUDHEIR A., TONTIWACHWUTHIKUL P., CHAKMA A., IDEM R.: *Kinetics of the reactive absorption of carbon dioxide in high CO₂-loaded, concentrated aqueous monoethanolamine solutions*. Chem. Eng. Sci. **58**(2003), 5195–5210.
- [16] VAIDYA P.D., KENIG E.Y.: *CO₂-alkanolamine reaction kinetics: A Review of recent studies*. Chem. Eng. Technol. **30**(2007), 11, 1467–1474.
- [17] FAIZ R., AL-MARZOUQI M.: *Mathematical modelling for the simultaneous absorption of CO₂ and H₂S using MEA in hollow fiber membrane contractors*. J. Membrane Sci. **324**(2009), 269–278.
- [18] *ANSYS FLUENT 13.0, User's Guide*. Lebanon, 2010.
- [19] FERZIGER J.H., PERIC M.: *Computational Methods for Fluid Dynamics*. Springer-Verlag Berlin Heidelberg New York, 2002.
- [20] *GAMBIT 2.4, User's Guide*. Lebanon, 2007.
- [21] NIEGODAJEW P., ASENDRYCH D.: *Modeling countercurrent gas-liquid flow in porous media*. Modelowanie Inżynierskie **14**(2012), 45, 108–115.
- [22] GASPARD J., CORMOS A-M.: *Dynamic modelling and validation of absorber and desorber columns for post-combustion CO₂ capture*. Comput. Chem. Eng. J. **35**(2010), 2044–2052.
- [23] MOSER P., SCHMIDT S., SIEDER G., GARCIA H., STOFFREGEN T.: *Performance of MEA in long-term test at the post-combustion capture pilot plant in Niederaussem*. Int. J. Greenh. Gas Con. **5**(2011), 620–627.